CAR20051082

CONTRIBUTIONS TO THE STUDY OF VEHICLE IMPACT AND POST-IMPACT DYNAMICS

[1]Preda, Ion* [1]Ciolan, Gheorghe, [1]Covaciu, Dinu, [1]Seitz, Nicolae, [1]Dima, Dragoş-Sorin
[1]Transilvania University of Braşov, Romania

KEYWORDS

accident reconstruction, post-impact dynamics, tyre behaviour, computer model, vehicle's speed estimation

ABSTRACT

The article presents the main stages necessary to reconstruct the impact of two vehicles.

A computer model, permitting to estimate the vehicle trajectories, was created. It was used to study the influence of different parameters over the accident dynamics.

MAIN SECTION

One of the most frequent traffic accident types is represented by the collision of two vehicles. When is demanded to analyse such a case, the technical expert studies the evidences found on the accident place and, based on his knowledge and experience, makes suppositions about the way the things happened. A computer program can be very helpful because, speeding up the calculations, permits to verify a big number of possible situations. So, the assumptions made can be infirmed or confirmed. Step by step, analysing the results and correcting errors, the expert approaches the scenario that better superposes the accident data.

In the following, based on results obtained by the help of simplified models, considerations regarding the dynamic behaviour of two vehicles involved in collision will be presented.

VEHICLES CRASH ASPECTS

When a crash happens, the vehicles' contact duration is normally very short (about a tenth-second) [14]. That means it is possible to neglect the influence of tyres friction and to approximate the reciprocal actions of the two vehicles as a shock consisting in an instantaneous transfer of energy. That phenomenon can be treated applying the two well known laws of mechanics [2]: energy conservation (Eq. 1) and impulse conservation (Eq. 2):

$$E_{1b} = E_{1d} + E_{1a} \qquad E_{2b} = E_{2d} + E_{2a} \qquad \text{Eq. 1}$$

$$m_1 v_{1b} + m_2 v_{2b} = m_1 v_{1a} + m_2 v_{2a} \qquad \text{Eq. 2}$$

In these equations, m represents mass, v – vehicle velocity, E – energy; the indices 1 and 2 associate with the two vehicles; the index d states for deformation; the indices b (before) and a (after) point out the preliminary moment and the succeeding moment of the impact.

Equation 1 shows in mathematical form that the before-crash energy ($E_{1b} + E_{2b}$) of the vehicles partly consumes in the bodies' deformations ($E_{1d} + E_{2d}$) and the remaining ($E_{1a} + E_{2a}$) determines the vehicles after-crash movements.

The energy of each vehicle is the summation of potential (depending on height) and kinetic (depending on velocity) energies [13]. For most of the accident situations, no important changes of centre of gravity height can occur. That means the energies before- and after-crash in Eq. 1 are only the kinetic energies of the vehicles.

Considering a plane model, as in figure 1, the kinetic energy of the vehicle is the sum of the **translational energy**

$$E_t = m\, v^2 / 2 \qquad \text{Eq. 3}$$

and the **rotational energy**

$$E_r = J\, \omega^2 / 2, \qquad \text{Eq. 4}$$

where J [$kg\ m^2$] is the moment of inertia over the rotation axis and ω [rad/s] is the yaw speed of the body.

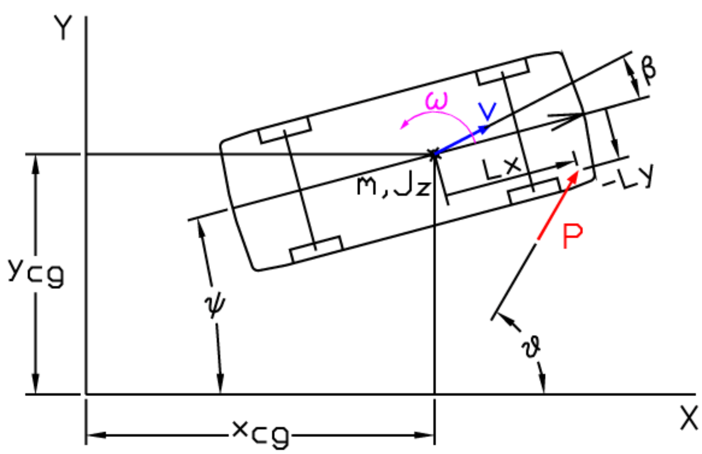

Fig. 1 Schema of forces acting on the road train during travel

The **percussion** (or impulse) defines as the integral of the impact force F in the impact interval 2τ:

$$P = \int_{tc-\tau}^{tc+\tau} F\, dt = F_{med}\, 2\tau \qquad \text{Eq. 5}$$

and represents the **momentum variation** of the vehicle [1], [2].

If accepts the hypothesis of a linear increase of the force followed by a linear decrease, then the maximal impact force is

$$F_{max} = 2\, F_{med} = P / \tau \qquad \text{Eq. 6}$$

where τ is half of the impact time.

The magnitude and the direction of the percussion vector $\vec{P}$ can be initially estimated considering the deformation shapes and the amplitudes of both vehicles bodies and using data from the literature that presents results of experimental tests [4], [10], [14] or crash simulations realised with the finite element method [8]. The deformation shape permits also to approximate the place where the percussion vector acts on the vehicle – for example in the centroid of the damaged area [7].

In figure 1 considers a vehicle, of mass m and moment of inertia J_z, having a certain position in a fixed coordinate system, given by the centre of gravity **coordinates** x_{cg}, y_{cg} and the **heading angle** ψ. On this vehicle, travelling with the velocity v and yawing with the speed ω_z, acts the percussion of magnitude P and orientation θ in a point of coordinates L_x and $-L_y$ measured in a mobile coordinate system linked to the vehicle's centre of gravity (that respects the ISO convention).

In the fixed coordinate system XOY, the percussion action modifies the two translational velocities v_X, v_Y and the yaw speed ω_Z with the amounts:

$$\Delta v_X = \frac{P\cdot\cos(\theta)}{m} \qquad \Delta v_Y = \frac{P\cdot\sin(\theta)}{m} \qquad \Delta\omega_z = \frac{P\cdot\left(L_x\cdot\sin(\theta-\psi) - L_y\cdot\cos(\theta-\psi)\right)}{J_z} = \frac{P\cdot d}{J_z}$$

$$\Delta v = \sqrt{\Delta v_X^{\,2} + \Delta v_X^{\,2}} = \frac{P}{m} \qquad \textit{Eq. 7}$$

with

$$d = L_x\cdot\sin(\theta-\psi) - L_y\cdot\cos(\theta-\psi) \qquad \textit{Eq. 8}$$

the distance between the percussion vector and the centre of gravity.

The percussion's application point in conjunction with his orientation determines how the vehicle changes his movement, more precisely how are modified the rotational and translational components of speed and energy.

Considering the **radius of gyration**

$$J_z = m\cdot r_g^{\,2} \qquad r_g = \sqrt{\frac{J_z}{m}} \qquad \textit{Eq. 9}$$

defines a ratio of impact rotational speed change and translational speeds change

$$\eta_v = \left|\frac{\Delta\omega_z\cdot r_g}{\Delta v}\right| = \left|\frac{\dfrac{P\cdot\left(L_x\cdot\sin(\theta-\psi)-L_y\cdot\cos(\theta-\psi)\right)}{m\cdot r_g}}{\dfrac{P}{m}}\right| = \left|\frac{d}{r_g}\right| \qquad \textit{Eq. 10}$$

and, similarly, the ratio of rotational energy change and translational energy change

$$\eta_E = \frac{\Delta E_r}{\Delta E_t} = \frac{J_z\cdot\Delta\omega_z^{\,2}}{m\cdot\Delta v^2} = \frac{r_g^{\,2}\cdot\Delta\omega_z^{\,2}}{\Delta v^2} = \eta_v^{\,2} = \left(\frac{L_x\cdot\sin(\theta-\psi) - L_y\cdot\cos(\theta-\psi)}{r_g}\right)^2 = \left(\frac{d}{r_g}\right)^2 \qquad \textit{Eq. 11}$$

Null value for one of these ratios is equivalent to

$$\eta_v = 0 \qquad d = 0 \qquad L_x\cdot\sin(\theta-\psi) = L_y\cdot\cos(\theta-\psi) \qquad \tan(\theta-\psi) = \frac{L_y}{L_x} \qquad \textit{Eq. 12}$$

and means the support of percussion vector pass thru the vehicle's centre of gravity and no change in rotational speed produces.

Using the value of η_v and η_E, easily computes the fraction represented by the rotational energy variation ΔE_r in the total (kinetic) energy variation ΔE:

$$\frac{\Delta E_r}{\Delta E} = \frac{\Delta E_r}{\Delta E_t + \Delta E_r} = \frac{\Delta E_t \cdot \eta_E}{\Delta E_t + \Delta E_t \cdot \eta_E} = \frac{\eta_E}{1 + \eta_E}$$

Eq. 13

This last equation shows the way that the impact energy distributes in two parts that modify (increasing or decreasing) the translational and rotational energies.

Because in the collision a part of kinetic energy consumes to crash the vehicles bodies, it is necessary to introduce the so called **restitution coefficient** defined as:

$$k = \frac{v1_a - v2_a}{v2_b - v1_b}$$

Eq. 14

Equations 2 and 14 permit to obtain two velocities if know the other two and the restitution coefficient. For that, the value *k* is adopted or, better, is computed from the value of deformation energy, estimated by other methods [4], [10], [14].

Introducing the notion of **inertance** [15]

$$g = \frac{1}{m} + \frac{d^2}{J_z}$$

Eq. 15

the deformation energy expresses as

$$E_d = E1_d + E2_d = \frac{(v1_b - v2_b)^2}{2} \cdot \frac{(1 - k^2)}{(g_1 + g_2)} = \frac{(v2_a - v1_a)^2}{2 \cdot k^2} \cdot \frac{(1 - k^2)}{(g_1 + g_2)}$$

Eq. 16

and permits to calculate the restitution coefficient

$$k = \sqrt{1 - \frac{2 \cdot E_d}{(v1_b - v2_b)^2} \cdot (g_1 + g_2)} = \frac{1}{\sqrt{1 - \frac{2 \cdot E_d}{(v2_a - v1_a)^2} \cdot (g_1 + g_2)}}$$

Eq. 17

To obtain the amounts that modify the velocity components Δv_X, Δv_Y and $\Delta \omega_z$ uses equation 7, considering the angle θ for the vehicle "1", respectively the angle $\theta+\pi$ for the vehicle "2".

MODEL OF TYRE

The key elements in the vehicle post-impact dynamics are the **tyres**. Three physical mechanisms contribute to the generation of the wheel-ground interaction force, better known as the **friction force**:

- **adhesion**, that arises (in the dimensional range of 1 nm to 1 μm) from the intermolecular bonds between the rubber and the aggregate in the road surface, producing shear stresses;
- **hysteresis**, that means the appearance of a force in the contact patch due to the supplementary energy loss in the rubber as it deforms to cover the road irregularities (in the range of 10 μm to 1 mm) when a (driving or braking) torque or a lateral force are applied to the tyre or when the wheel is steered (changing his orientation with respect to his displacement direction);

- **soil resistance to the distortion**, that produces (in the macro dimensional range) only when the ribs of the wheel engage the soft (deformable) ground or the hard ground's large irregularities.

To generate tyre-ground friction force, two elements must exist:

- **normal load**, a force that presses the tyre against the ground;
- **tyre slip** (or at least a tendency to slip).

If one of these two is missing, no friction force produces.

Practically, the friction force can reach in any direction the same maximal absolute value, the **peak friction force**, which can be computed with the equation

$$F_{max} = \mu_P \; Z \qquad \textit{Eq. 18}$$

where Z is the normal load of the tyre and μ_P is the **peak friction coefficient** that indicate the best grip properties in a given tyre-ground interface.

It considers a mobile coordinate system $x_w C_{cp} y_w$ attached to the centre of wheel contact patch and having the semi-axis x_w pointing forward in the wheel's longitudinal plane, figure 2. During movement, the tyre's point in the centre of contact patch has the **theoretical** (rolling) **velocity** $v_t = \Omega\, r_d$ (with Ω the rotating speed of the wheel and r_d – the dynamic radius of the wheel) that has as support the semi-axis x_w. The wheel's **real velocity** v makes with the vector v_t (and semi-axis x_w) the **slip angle** α. The vectorial difference $\vec{v}_s = \vec{v} - \vec{v}_t$ represents the **slip velocity** that the wheel slides on the ground. The real velocity and the slip velocity can be also considered as resultant of their components:

$$\vec{v} = \vec{v}_t + \vec{v}_s = \vec{v}_x + \vec{v}_y \qquad \vec{v}_s = \vec{v}_{sx} + \vec{v}_{sy} \qquad \textit{Eq. 19}$$

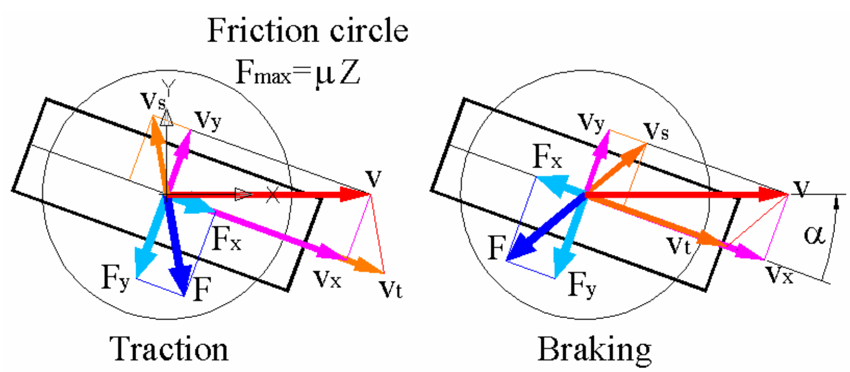

Fig. 2 Velocities and friction forces in the tyre-ground contact patch (upper view, right turn)

The **actual friction force** $\vec{F}$ acting on tyre has the same support as the slip velocity vector, but opposite orientation (the force opposes to the slip). His magnitude depends on the peak friction force and on the tyre's **total slip** s, defined as

$$s = v_s / v_x = \sqrt{\kappa^2 + tg^2\alpha} \qquad \textit{Eq. 20}$$

The components of the total slip are the longitudinal slip κ:

$$\kappa = v_{sx}/v_x = \begin{cases} 1 - \dfrac{v_x}{v_t} & if \quad v_x < v_t \\ 0 & if \quad v_x = v_t \\ -\left(1 - \dfrac{v_t}{v_x}\right) & if \quad v_x > v_t \end{cases} \qquad \textit{Eq. 21}$$

and the lateral slip

$$tg\alpha = v_{sy} / v_x \qquad Eq.\ 22$$

with α the slip angle.

Figure 3 shows a typical representation of the **relative friction coefficient** (indicating the fraction of $F_{\max}$ that is generated in the contact patch)

$$\xi = F / F_{max} \qquad Eq.\ 23$$

as a function of total slip s. In the ISO convention, considers positive values for s and ξ during traction and negative for braking.

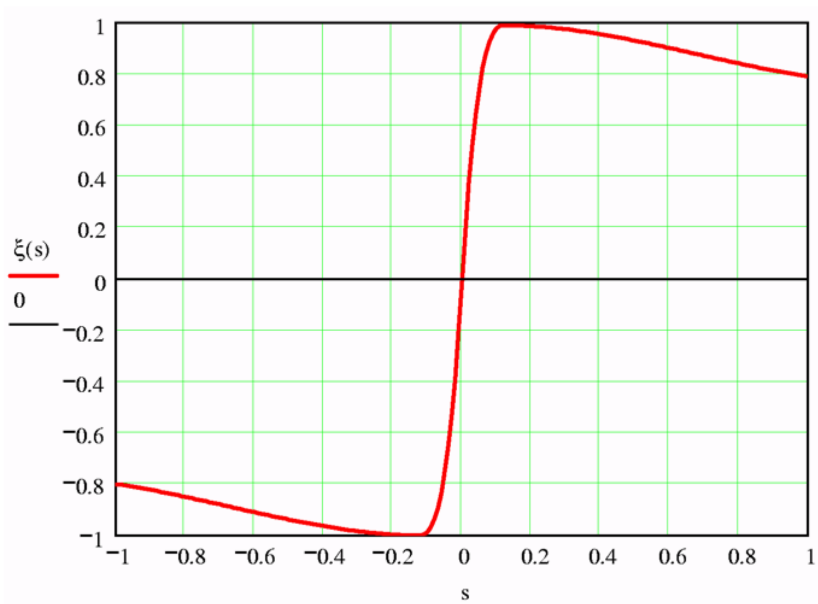

Fig. 3 Tyre's actual friction coefficient vs. total slip

The **(**actual) **friction coefficient** μ (also called "used friction") and the tyre's **(**actual) friction force F are

$$\mu = \mu_P\, \xi \qquad F = \mu\, Z = \mu_P\, \xi\, Z = \xi\, F_{max} \qquad Eq.\ 24$$

The curve $\xi(s)$ has two important domains for both traction and braking

- the domain of small slip, also named **pseudo-slip** (s < 0.05…0.1), characterised by the absence of slide in the contact patch; the appearance of slip come for the elastic deformation under stress of tyre material;
- the domain of evident slip, characterised by the existence of slide in the contact patch, phenomenon evidenced by black tyre marks on hard grounds; if |s|=1, the slide appears in any point of the contact patch (s=1 means the wheel spins but no wheel translation produces; s=-1 means the wheel is locked but continue to translate); when slide occurs only in a small area of the contact patch (normally, in the field 0.1<|s|<0.3), the absolute friction force takes the biggest values.

To mathematically model the shape of $\xi(s)$ curve, many formulae, more or less empirical, were suggested [3], [5]. Anyway, this shape is defined well enough by only some quantities:

- the slope at the origin, proportional to the tyre stiffness;
- the slip value s_P that corresponds to the maximal grip (μ_P, F_{max});

- the value of the friction coefficient μ_S that corresponds to the total slip (s=1 or s=-1) and the slope of the curve in the area of total slip.

MODEL OF INTEGRAL ACTION OF THE WHEELS

The friction forces of all the wheels and the grade and aerodynamic resistances produce continuous variations of the dynamic load Z of each wheel. Also, the impact it self, dramatically changes the dynamic loads (in comparison with the static ones) at the beginning of the post-impact phase. The computation of these loads can be performed using quasi-static [9], [11], [16] or dynamic [6], [11] suspension models that include pitch and roll degrees of freedom.

If desired, even the change of the wheel's dynamic radius r_d under variable load can be also considered [5].

To control the friction force of the tyre, two possibilities exist:

- to modify the longitudinal slip κ by the application of a driving or braking torque that accelerates or brakes the wheel spinning and implicitly change the theoretical velocity v_t;
- to modify the lateral slip tgα by steering the wheel, i.e. changing his position relative to the real velocity v (the angle α**).**

To be able to compute the friction force of a certain wheel it is necessary to know the dynamic load, the peak friction coefficient and the orientation and magnitude of two vectors: real and theoretical velocities.

The real velocity of a contact patch centre computes adding the velocity associated to the yaw speed to the velocity $\vec{v}_{cg}$ of the vehicle's centre of gravity (fig. 1):

$$\vec{v} = \vec{v}_{cg} + \vec{\omega}\,\vec{d}_w \qquad \textit{Eq. 25}$$

where $\vec{d}_w$ represent the distance vector between the centre of gravity and the middle of the contact patch.

To compute the other velocity, the theoretical one, it is necessary to simulate the functioning of the driving and braking systems [12] or to make some assumptions about the longitudinal slip κ or about the magnitude of the longitudinal force F_x.

Important simplifications can be made if considers two extreme cases. The first one considers a **free wheel** (no torque is applied), specific to a car out of control (injured driver). In this situation, the friction coefficient is equal with the rolling resistance coefficient, $\mu=-f$ and the longitudinal slip κ is very small and can be neglected.

The second case considers a **locked wheel** under the effect of a panic braking. This means that $\kappa=-1$ and $\mu=\mu_S$, the value that corresponds to the total slip.

The wheel slip angle α_w computes with the equation (fig. 1 and fig. 2)

$$\alpha_w = \mathrm{arctg}\left(\frac{v_{wy}}{v_{wx}}\right) - \left(\psi + \delta_w\right) \qquad \textit{Eq. 26}$$

as function of the longitudinal and transversal components (v_{wx}, v_{wy}) of the real velocity, the actual heading angle ψ and the wheel steering angle δ_w.

Now, with the equations 19-22 determines the vector $\vec{v}_s$, then the orientation and the magnitude of the friction force $F=f(\mu_P,\xi,Z)$ and finally his components in tangential and lateral direction

$$F_x = \frac{\kappa}{\sqrt{\kappa^2 + tg^2\alpha}}\ F_{\max} \qquad F_y = \frac{tg\alpha}{\sqrt{\kappa^2 + tg^2\alpha}}\ F_{\max} \qquad \text{Eq. 27}$$

Now, using the forces of all the wheels, it is possible to write the system of three equations that defines the vehicle's dynamical behaviour (in the fixed coordinate system) during the after-impact period:

$$a_X = \frac{\Sigma\left(X_w\cdot\cos(\psi + \delta_w) - Y_w\cdot\sin(\psi + \delta_w)\right)}{m}$$

$$a_Y = \frac{\Sigma\left(X_w\cdot\sin(\psi + \delta_w) + Y_w\cdot\cos(\psi + \delta_w)\right)}{m}$$

$$\begin{aligned}\varepsilon_Z = {} & \frac{\left(Y_{fl}\cdot\cos(\delta_{fl}) + X_{fl}\cdot\sin(\delta_{fl}) + Y_{fr}\cdot\cos(\delta_{fr}) + X_{fr}\cdot\sin(\delta_{fr})\right)\cdot L_a}{J_Z} \ldots \\ & + \frac{\left(-Y_{rl}\cdot\cos(\delta_{rl}) - X_{rl}\cdot\sin(\delta_{rl}) - Y_{rr}\cdot\cos(\delta_{rr}) - X_{rr}\cdot\sin(\delta_{rr})\right)\cdot L_b}{J_Z} \ldots \\ & + \frac{\left(Y_{fl}\cdot\sin(\delta_{fl}) - X_{fl}\cdot\cos(\delta_{fl}) + Y_{rl}\cdot\sin(\delta_{rl}) - X_{rl}\cdot\cos(\delta_{rl})\right)\cdot\frac{E}{2}}{J_Z} \ldots \\ & + \frac{\left(-Y_{fr}\cdot\sin(\delta_{fr}) + X_{fr}\cdot\cos(\delta_{fr}) - Y_{rr}\cdot\sin(\delta_{rr}) + X_{rr}\cdot\cos(\delta_{rr})\right)\cdot\frac{E}{2}}{J_Z}\end{aligned} \qquad \text{Eq. 28}$$

Then, numerically integrating these equations, obtains the velocities (v_X, v_X, ω) and the displacements (s_X, s_X, ψ) of the vehicle's centre of gravity.

To help the use of the algorithm, a computer program was realised that permits to graphically represent different vehicles in their computed successive positions. For that, a database with bi- or tri-dimensional CAD models was designed and is continuously increasing by adding new models.

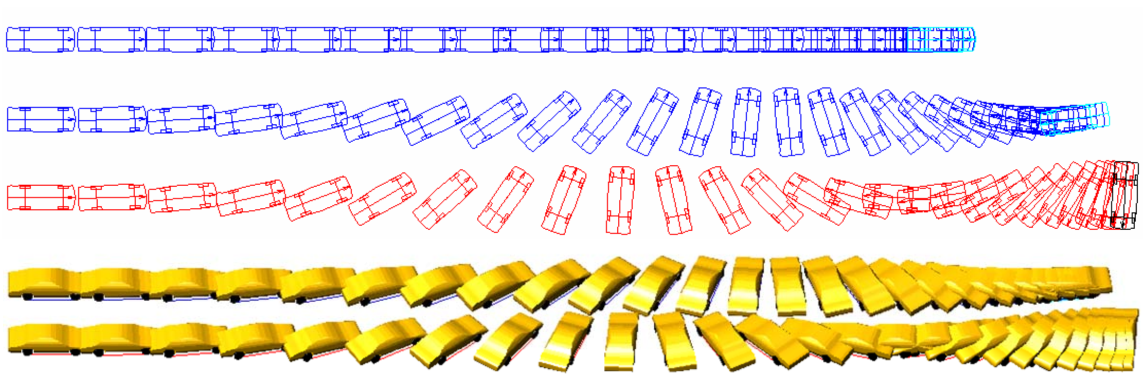

Fig. 4 Simulation of braking with locking wheels: up – homogenous surface (μ=0.8) middle – μ-split condition (μ_{hi}=0.8, μ_{lo}=0.45); bottom – μ-split condition (μ_{hi}=0.8, μ_{lo}=0.1)

As an example of algorithm and graphic program possibilities, in figure 4 presents the case of a car that brakes from 108 km/h with all wheels locked. No steering angle is applied to the front wheels before and during braking. Three situations were considered: a homogenous road surface (μ=0.8) and two μ-split conditions, with the same higher friction coefficient μ_{hi}=0.8 (on the left side) but different lower values: μ_{lo}=0.45, respectively μ_{lo}=0.1.

The program permits to assign different frictional properties for different areas of the ground, including gradual transitions for a value to other.

The picture shows successive vehicle plots made at equal time interval of 0.2 s. The data for these situations is (total stopping time, distance and gyration angle):

- 3.8 s; 57.4 m; vehicle maintains his initial orientation;
- 4.2 s; 66 m; 186°
- 4.3 s; 69.8 m; 268°.

EXAMPLES OF POST-IMPACT STUDY

To exemplify the use of the theoretical elements previously presented further explains the way chosen by the authors to reconstruct a traffic accident. The data of the two vehicle implied in the collision is: mass – m_1=2700 kg, m_2=1160 kg; yaw moments of inertia – J_{z1}=4559 kg m^2, J_{z2}= 1711 kg m^2; wheelbase – L_1=2.6 m, L_2=2.441 m; longitudinal distance from the centre of gravity to the front axle – L_{f1}=1.26 m, L_{f2}=1.1 m; wheel track – E_1=1.65 m, E_2=1.312 m; coordinates of percussion application point (relative to the vehicle centre of gravity) – L_{x1}=2.19 m, L_{y1}=-0.55 m, L_{x2}=0.62 m, L_{y2}=0.776 m.

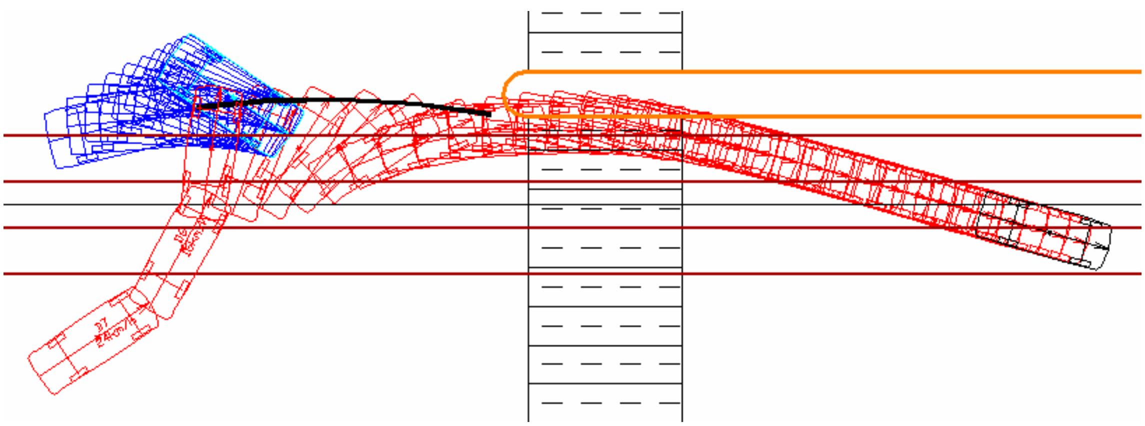

Fig. 5 Film of an accident post-impact phase
the vehicle "1" (blue) is braked; the vehicle "2" (red) is out of control

Successive vehicles positions during impact and post-impact are represented in figure 5 (for all the process) and in figure 6 (as a detail). The existing data at the accident scene were:

- the final position of vehicle "1" (blue), represented in light blue;
- the final position of vehicle "2" (red), represented in black;
- a tyre slippage mark, represented in black;
- the information that the vehicle "2" was stopped when it was hit and that the driver have lost his knowledge because the shock.

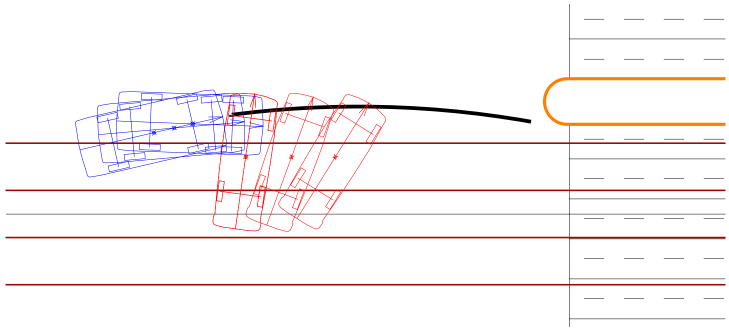

Fig. 6 Three successive vehicles' positions at 0.2 s time interval
the left side vehicle (2700 kg): 30→13 km/h; the right side vehicle (1160 kg): 0→27 km/h
percussion magnitude: 8861 N.s

For the reason that initial position estimation for the vehicle "2" was evident, due to the tyre slippage mark, it wasn't necessary to perform a "reverse kinematics" analysis in order to obtain a rough velocity estimation for the vehicle "2".

Furthermore, the method of "reverse kinematics" doesn't lead to good results because the rotational and translational energies are consumed by the tyres friction in different time intervals, that can't be determined if the analysis starts from the final position to the initial.

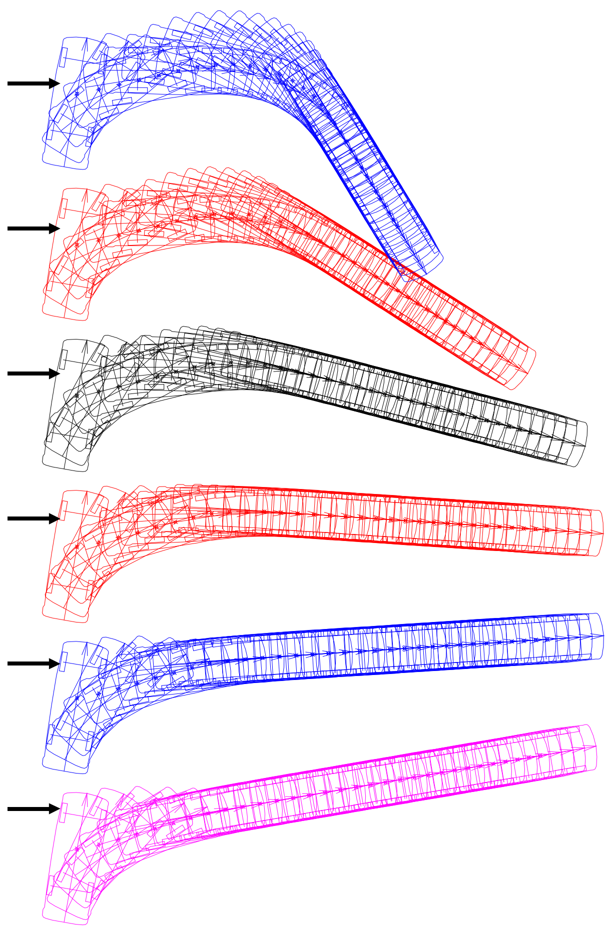

Fig. 7 The influence of the impact point on the post-impact trajectory and heading

Considering free wheels for vehicle "2", braked wheels for vehicle "1" and using the program repeatedly, it was found the percussion's best magnitude (8861 N.s) and application point for which the trajectory of the left-front wheel of vehicle "1" superposes better over the tyre slippage mark and assures the final positions of both vehicles.

As can be seen in figure 7, the post-impact vehicle trajectory and heading are very sensible on the position of the percussion application point. In the figure, the application point was moved with 0.2 m from case to case. The third case from top corresponds to the point determined after the crash deformation analyse and assures excellent concordance with the tyre mark and the final position.

Calculating a restitution coefficient of 0.85 and having now the after-impact velocities and yaw speeds of both vehicles, it obtains the others, before-impact: vehicle "1" is decelerated for 30 km/h to 13 km/h and vehicle "2" is accelerated for rest to 27 km/h.

CONCLUSIONS

This article focused on two stages of the reconstruction of a vehicle-vehicle traffic accident:

- the **impact**, considered as a collision of two planar bodies and governed by the laws of mechanics;
- the **post-impact movement**, considering the influence of each tyre in the vehicle trajectories.

Summarising, the main steps that must be performed in the study of such an accident are:

- a quantification of the deformation energy and an initial estimation of the percussion application point, orientation and magnitude, that can be done analysing the shape and profundity of the crash areas;
- an approximate inverse kinematics, based on the distances between the vehicles impact and stopping places, that permits to roughly appreciate the post-impact values of the velocities;
- using a simulation program, the expert tries to realise a fine match of the computed vehicles trajectories with the tyres marks and other evidences from the accident scene; when this succeeds, obtains the most probable values for impact exit velocities and percussion;
- based on the already computed deformation energy, determines the crash loss of speeds and then the impact entering velocities.

The presented algorithm, that permits to estimate with high probability the post-impact vehicle behaviour, can be used directly, as it is, or to be included in more sophisticated models, permitting to study many others aspects of vehicle dynamics, as traction, braking, stability or handling.

REFERENCES

(1) Untaru M., Poțincu Gh., Stoicescu A., Pereş Gh., Tabacu I. "Dinamica autovehiculelor pe roți" ("Dynamics of Wheeled Motor Vehicles"). Editura Didactică şi Pedagogică, Bucureşti, 1981.

(2) Olariu V., Sima P., Achiriloaie V. Mecanica tehnică (Technical Mechanics). Editura Tehnică, Bucureşti, 1982.

(3) Pacejka H., Bakker E. The magic formula tyre model. 1991.

(4) Baumler H. Energetische Betrachtungen zur Reconstruction von Verkehrsunfällen (Energetic view about traffic accident reconstruction). Verkehrsunfall und Fahrzeugtechnik 04/95, Heft 1.

(5) Preda I., Ciolan Gh. Modelarea interacţiunii dintre roată şi sol (Modelling of the wheel-ground interaction). The VIIth Automotive Conference CAR '97, vol.A, p.85-90, Piteşti.

(6) Pandrea N., Pârlac S., Popa D. Modele pentru studiul vibraţiilor automobilelor (Models for the study of vehicle vibrations). Editura TipArg, Piteşti, 2001.

(7) Mitchell J.F. International Guide Book for Traffic Accident Reconstruction. Actar, 2002.

(8) Tabacu Şt. Modele pentru studiul impactului frontal şi lateral la automobile de fabricaţie românească (Models for the frontal and lateral impact study of motor vehicles made in România). Doctoral Thesis, University of Piteşti, 2002.

(9) Preda I., Flueraş Al., Câmpian O. Bending torques on solid beam axle during cornering. Automotive International Congress ESFA 2003, p.271-276, Bucureşti.

(10) Pritzkow R. Cercetări energetice în coliziunile autoturismelor (Energetic researches on car collisions). Doctoral Thesis, Transilvania University of Braşov, 2003.

(11) Mitschke M., Wallentowitz H. Dynamic der Kraftfahrzeuge (Motor Vehicle Dynamics). Springer-Verlag, 2004.

(12) Preda I., Ciolan Gh., Dogariu M., Todor I. Computer model to simulate the vehicle longitudinal dynamics. The Xth International Automotive Congress "CONAT 2004", paper 1060, Braşov, 2004.

(13) Ciolan Gh., Preda I., Covaciu D. Accident reconstruction example – A possible modality for rollover "after the fact" study. The Xth International Automotive Congress "CONAT 2004", paper 2069, Braşov.

(14) Pritzkov R., Seitz N., Ciolan Gh., Preda I., Enache V., Dima D. Evaluarea diagramelor crash-testelor în vederea determinării rigidităţii caroseriilor (Crash-tests diagrams evaluation to determine the stiffness of vehicle bodies). Session of technical experts. Căciulata, Romania, 2005.

(15) Pandrea N. The classical model of two solids collision. 1st International Conference "Computational Mechanics and Virtual Engineering" COMEC 2005, Braşov.

(16) Preda I. Aspects regarding the wheel loads of tractor-semitrailer road train. The IXth Automotive International Congress "CAR 2005", paper 1114, Piteşti.